

# On hidden twin attractors and bifurcation in the Chua's circuit

Qingdu Li · Hongzheng Zeng · Xiao-Song Yang

Received: 17 October 2013 / Accepted: 30 January 2014 / Published online: 19 February 2014  
© Springer Science+Business Media Dordrecht 2014

**Abstract** Recently a new attractor, called hidden attractor, has been found in the well-known Chua's circuit, whose basin of attraction does not contain neighborhood of any equilibrium. This paper will restudy this circuit, showing that two hidden attractors can coexist in this circuit for some parameters, and characterizes the basins of these two attractors by means of computer method as well. In addition, a computer-assisted proof of the chaoticity of these attractors is presented by a topological horseshoe theory.

**Keywords** Hidden attractor · Topological horseshoe · Chua's circuit · Poincaré map

## 1 Introduction

In many dynamical systems such as Lorenz [1], Rössler [2], Chua [3,4] and Chen [5] systems, the attractors well known in these systems can usually be found by tracing an unstable manifold from some equilibrium. For example, since the strange attractors called Chua's

attractors was discovered in Chua's circuit, all the well-known Chua's attractors to date have been the attractors that are excited from some unstable equilibria. From computational point of view, this allows one to use numerical methods in identifying attractors through a trajectory started from a point on a local unstable manifold of some saddle type equilibrium.

Recently Leonov and Kuznetsov [6,7] reported a remarkable result at plenary lecture in PhysCon 2009: an interesting phenomenon called as "the hidden attractor" can take place in the Chua's circuit. Further development of these studies was presented by their group in a number of papers [8–10] and the review article [11]. The so called hidden attractor, according to Leonov et.al, means an attractor having a basin of attraction which does not intersect with small neighborhood of any equilibrium. Therefore, hidden attractors are different from that ones known before [4], and cannot be localized by standard computational procedures mentioned previously, thus investigation of such attractors is a much more difficult problem.

Motivated by the work [6], the aim of the present paper is twofold. First we re-investigate the hidden attractor reported by [6], and show that in fact two hidden attractors, hidden twin attractors, as called in the present paper, can be found in the Chua's circuit, a little more interesting phenomenon observed in Chua's circuit. Then we study the bifurcations related to the hidden twin attractors, and present computer studies on the attraction basin of these two hidden attractors. Finally,

---

Q. Li · H. Zeng · X.-S. Yang (✉)  
Key Laboratory of Industrial Internet of Things &  
Networked Control, Ministry of Education, Chongqing  
University of Posts and Telecommunications,  
Chongqing 400065, China  
e-mail: yangxs@mail.hust.edu.cn

X.-S. Yang  
Department of Mathematics, Huazhong University of Science  
and Technology, Wuhan 430074, China

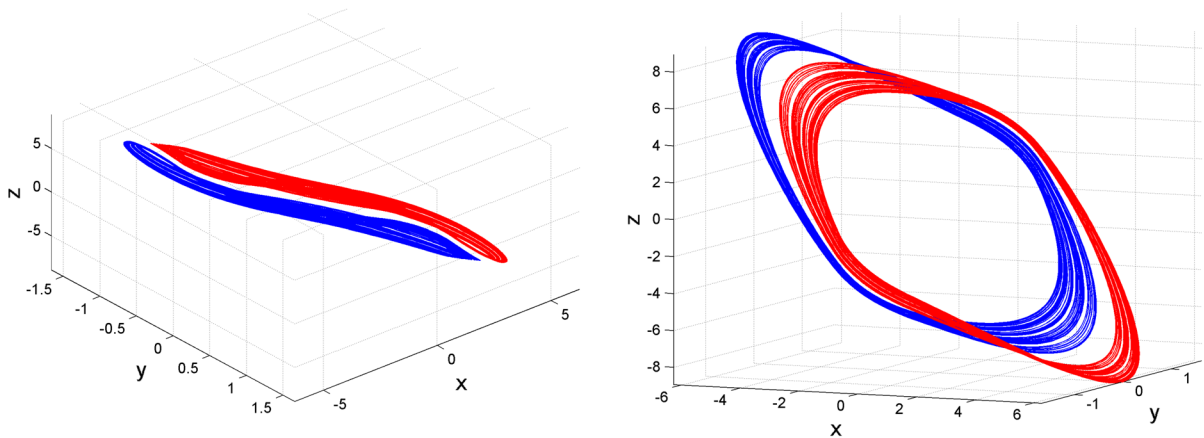


**Fig. 1** The hidden twin attractors in the Chua’s circuit with different view angles

we give a computer-assisted proof of existence of topological horseshoe exhibited in these attractors.

## 2 The hidden attractor and its bifurcation

In this section, we will study the hidden attractors and related bifurcations.

### 2.1 Hidden twin attractors

Chua’s circuit can be described by the following differential equations in dimensionless coordinates:

$$\begin{aligned} \dot{x} &= \alpha(y - x) - \alpha f(x) \\ \dot{y} &= x - y + z, \\ \dot{z} &= -\beta y - \gamma z \end{aligned} \tag{1}$$

where the function

$$f(x) = m_1 x + \frac{1}{2}(m_0 - m_1)(|x + 1| - |x - 1|), \tag{2}$$

characterizes the nonlinearity of Chua’s diode;  $\alpha$ ,  $\beta$ ,  $\gamma$ ,  $m_0$ , and  $m_1$  are parameters of the system. Recently, Leonov et al.’s reported in [6] that there is a hidden attractor when the parameters take as follows:

$$\begin{aligned} \alpha &= 8.4562, & \beta &= 12.0732, & \gamma &= 0.0052, \\ m_0 &= -0.1768, & m_1 &= -1.1468. \end{aligned} \tag{3}$$

The initial condition they gave to trace this attractor is  $x(0) = 9.4287$ ,  $y(0) = 0.5945$ ,  $z(0) = -13.4705$ .

To reproduce the phase portrait of the hidden attractor with higher precision, we utilize the fourth–fifth-order

Runge–Kutta method, and compute basin of attraction carefully with the heterogeneous algorithm proposed in [12, 13], based on the analytical result in [6].

Surprisingly, our computation suggests that there are two different hidden attractors instead of one, as shown in Fig. 1. The left subfigure is a side view, and shows a clear gap between the two attractors, so they are indeed separated from each other. The right subfigure depicts the detailed shapes with a front view, and suggests that they look similar to each other. Since system (1) is invariant under the transformation

$$(x, y, z) \leftrightarrow (-x, -y, -z), \tag{4}$$

the two attractors must be symmetric to each other with respect to the origin. The new initial conditions we used here are

$$x(0) = -6.0489, \quad y(0) = 0.0839, \quad z(0) = 8.7739$$

and

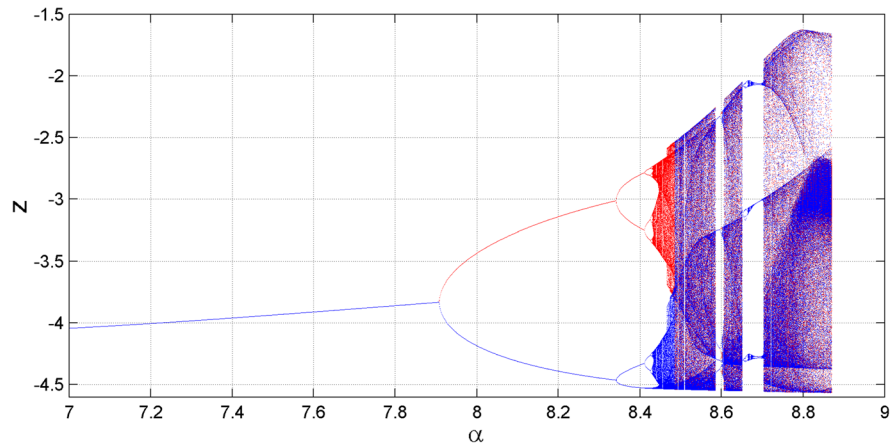
$$x(0) = 6.0489, \quad y(0) = -0.0839, \quad z(0) = -8.7739,$$

which lead to hidden attractor 1 (in blue color) and hidden attractor 2 (in red color), respectively.

Comparing with the simulations in [6], each attractor in Fig. 1 is clearly different from the one reported in [6]. In fact two hidden attractors do exist in this circuit. For convenience we call them hidden twin attractors in the present paper, since the two attractors look similar to each other.

This evidence inspires us three interesting questions: (i) where do the two hidden attractors come from; (ii) can the two attractors join together by adjusting a parameter; (iii) what do their basins of attraction look like?

**Fig. 2** The bifurcation diagram as we adjust  $\alpha$



In what follows, we will study the bifurcation diagram, basins of attraction, and Lyapunov exponents (LE) with varying  $\alpha$  from 7.0 to 9.0 while the other parameters take the same values as in (3) so that we can easily compare our results with [6].

To compute bifurcation diagrams and basins of attraction, we conveniently study a Poincaré map defined on a suitable cross section. The cross-section plane is taken as

$$P = \{(x, y, z) \mid x = 0, \dot{x} < 0\}$$

According to (1),  $P$  is actually the half  $yo$  $z$ -axis plane with negative  $y$ , i.e.,

$$P = \{(x, y, z) \mid x = 0, y < 0\},$$

since  $\alpha$  is always taken a positive number. The reason why we take  $x = 0$  instead of the switching manifold  $x = \pm 1$  is because the system is symmetric with respect to the origin, so we can easily extend our results to the full  $yo$  $z$ -axis plane. Then the corresponding Poincaré map is defined as: For each  $\mathbf{x} = (x, y, z) \in P$ ,  $h(\mathbf{x})$  is taken to be the first return point in  $P$  under the flow with the initial condition  $\mathbf{x}$ . The first accurate numerical method for computing Poincaré maps of Chua’s circuit was done by Lozi and Ushiki [14], which led to precise numerical analysis of bifurcations and attractors (and coexistence on attractors).

### 2.2 Hidden twin attractors by period-doubling bifurcations

This subsection will show another interesting phenomenon in the Poincaré map that the hidden twin attrac-

tors in Fig. 1 actually come from ONE period-1 limit cycle. First, this limit cycle bifurcates into two different period-1 limit cycles, and then the two limit cycles become two different chaotic attractors via period-doubling bifurcations, respectively. This fact seems different from the usual route of period-doubling bifurcations to chaos, and will be discussed in detail in Sect. 3 in addition to the following arguments.

To compute a bifurcation diagram, we trace the two hidden attractors for  $\alpha \in [7.0, 9.0]$ , respectively. The results are shown in Fig. 2, where the lower branch (in blue color) is shown in the diagram from hidden attractor 1, and the upper branch (in red color) depicts numerical output from hidden attractor 2. In order to classify the complex behaviors in Fig. 2, we compute their LE, as shown in Fig. 3. This figure not only suggests that the hidden attractor in Fig. 1 is chaotic, but also shows more limit cycles and chaotic behaviors, which will be studied in detail in what follows. It was noted that positive LE is not always indication of chaos [15, 16]; therefore we remain the rigorous study on chaos by means of the topological horseshoe theory in the next section.

The global picture of Fig. 2 may give the readers a false impression that it is simply a reverse period-doubling route to chaos. However, if we investigate Fig. 2 very carefully, then we may find an interesting bifurcation phenomenon not yet reported in the literature.

For  $7.0 \leq \alpha < 7.907$ , there are one zero and two negative LE in Fig. 3, and the system exhibits only one limit cycle with period-1 in Fig. 2. A typical phase portrait is shown in the left-top subfigure in Fig. 4 with  $\alpha = 7.8$ . When  $\alpha \approx 7.907$ , the limit cycle meets a

**Fig. 3** Lyapunov exponents as we adjust  $\alpha$

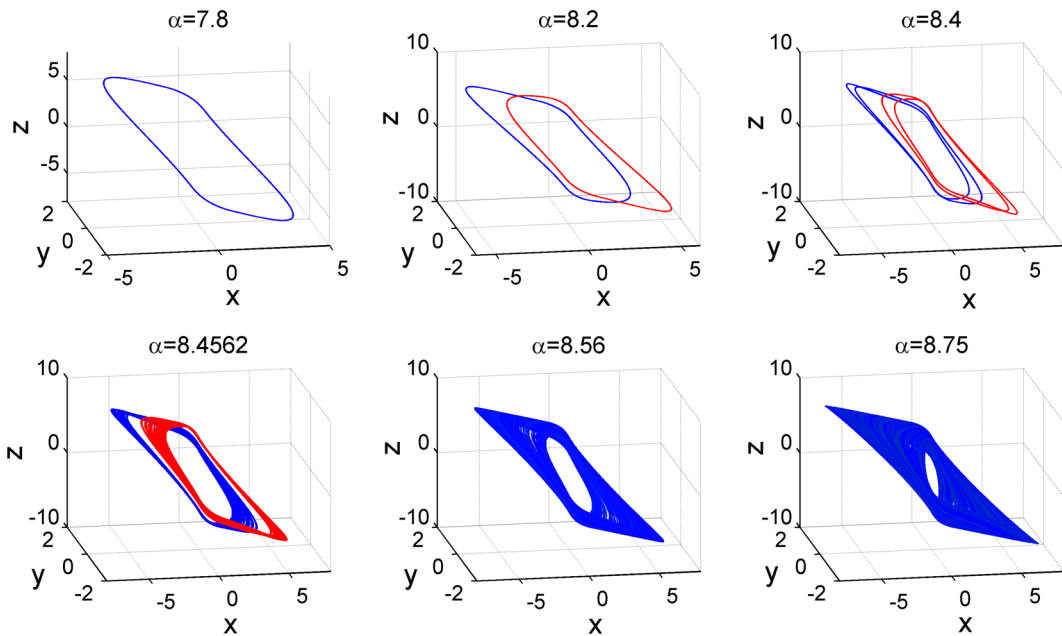
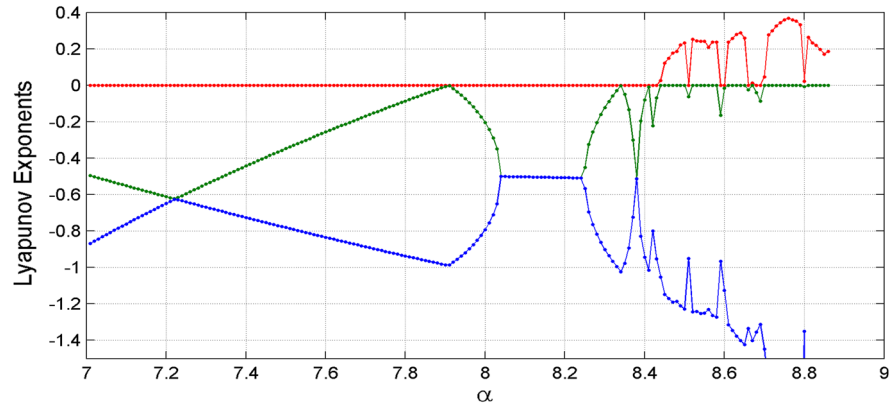


**Fig. 4** Typical phase portraits as we adjust  $\alpha$

bifurcation point in Fig. 2, and the second LE increases to zero in Fig. 3. For  $7.907 < \alpha < 8.341$ , we observe that the period-1 limit cycle bifurcates into two different period-1 limit cycles, as shown in different colors in Fig. 2. Both of the limit cycles have one zero and two negative LE. According to (4), they are symmetric to each other with respect to the origin. And a typical phase portrait at  $\alpha = 8.2$  is shown as the mid-top subfigure in Fig. 4. When  $\alpha$  continuously grows from 8.341, both of the limit cycles become period-2 limit cycles via a period-doubling bifurcation, as shown in Figs. 2 and 3. Two typical such cycles are shown in the right-top subfigure in Fig. 4 at  $\alpha = 8.4$ , respectively.

The bifurcation at is quite different from the common period-doubling bifurcation at  $\alpha = 8.341$ . To find what kind of bifurcations takes place, we compute the eigenvalues of the Jacobian matrix of the Poincaré map  $h$  along the limit cycles. The eigenvalues for the bifurcation at  $\alpha = 7.907$  is illustrated in Fig. 5, where the (blue) thin dot line indicates the period-1 orbit after the bifurcation, and the (green) bold solid and dot lines indicate the absolute eigenvalues before and after the bifurcation, respectively. The result for the bifurcation at  $\alpha = 8.341$  is illustrated in Fig. 6 in the same way. The two figures suggest both of the bifurcations are the Pitchfork bifurcation, i.e., one of the two eigenvalues

**Fig. 5** Bifurcation at  $\alpha = 7.907$  and the eigenvalues

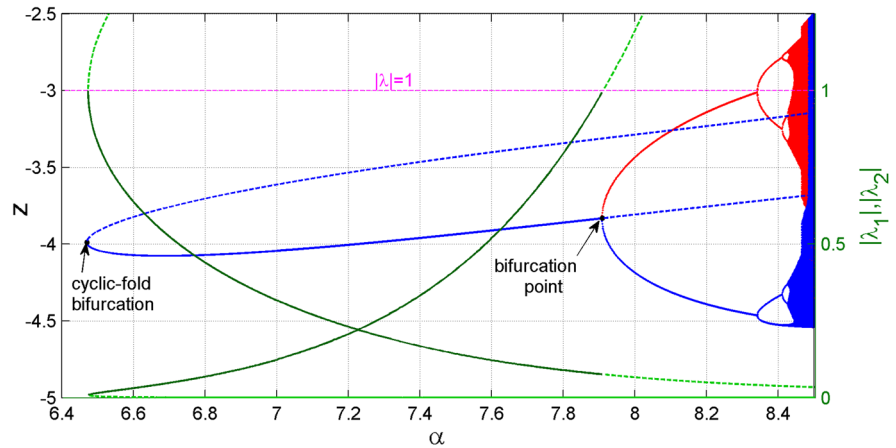
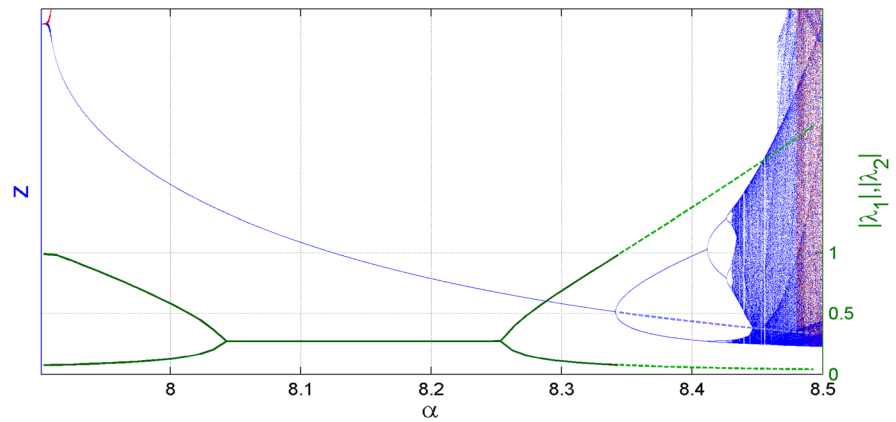


**Fig. 6** Bifurcation at  $\alpha = 8.341$  and the eigenvalues



crosses the unit circuit from inside to outside while the limit cycles become unstable after the bifurcation.

Since these bifurcations start with the stable single-loop limit cycle, it is necessary to find where it is from. This kind of stable limit cycles usually arise at a supercritical Hopf bifurcation, e.g., the systems discussed in [17, 18]. However, when we trace it from  $\alpha = 7.0$  via continuation method used in [19], we find a cyclic-fold bifurcation [20]. As shown in Fig. 5, when  $\alpha$  decreases, there is also one absolute eigenvalue crossing the line  $|\lambda| = 1$ . At the crossing point  $\alpha \approx 6.470$ , the limit cycle just loses its stability without bearing new periodic orbits. Meanwhile, this unstable cycle turns back.

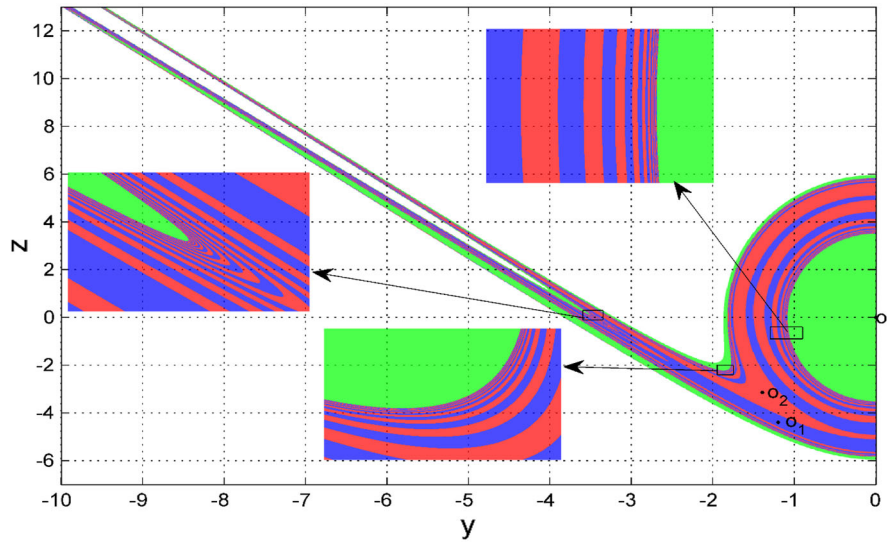
When  $\alpha$  continuously increases from 8.2, after a sequence of period-doubling bifurcations as depicted in Fig. 2, the two limit cycles lead to two different hidden chaotic attractors, respectively. A typical phase portrait of the attractors are shown in Fig. 1 and the left-bottom subfigure in Fig. 4, where  $\alpha = 8.4562$ . The three LE are 0.1124, 0.0000, and  $-1.1358$ , respec-

tively. It is interesting that a symmetric pair of stable single-loop limit cycles bifurcate into a symmetric pair of twin attractors in the three dimensional Chua's circuit. Similar bifurcation phenomenon has been found in seven dimensional systems [21, 22].

When  $\alpha$  continuously increases from 8.4562, Fig. 2 shows that the system exhibits abundant complex dynamics, and then becomes non-attractive when  $\alpha > 8.87$ . According to Fig. 2, the red dots and the blue dots are mixed together for  $\alpha > 8.486$ , which means that the two hidden attractors join together and become single hidden attractor as we expected. The single hidden attractor at  $\alpha = 8.56$  is illustrated in the mid-bottom subfigure in Fig. 4. It is also chaotic since the three LE are 0.2396, 0.0000, and  $-1.2753$ , respectively.

Further simulation suggests that when  $\alpha = 8.8$  the hidden attractor become an attractor that can be traced from the unstable manifold of the origin (the origin is now unstable at the given parameter). The normal attractor is shown in the right bottom subfigure in Fig. 4.

**Fig. 7** Basin of attraction at  $\alpha = 8.2$



The attractor looks very complicated, but the three LE are 0.0078,  $-0.0089$ , and  $-1.2422$ , respectively, which is hard to tell whether the attractor is chaotic or not. So we will study the chaocity in the next section by a topological horseshoe too.

### 2.3 Attraction basins of attractors

With the parameters used in the bifurcation diagram Fig. 2, system (1) has three equilibria: the origin and two symmetric saddles with respect to the origin. Similar to Leonov et al.’s computation in [6], each saddle has only one eigenvalue with a positive real part, and the attractors mentioned above cannot be traced from the corresponding unstable manifold. In order to check whether these attractors are hidden in the sense of [6], we need to study the stability of the origin with varying  $\alpha$  from 7.0 to 9.0, as well as their basins of attraction.

The Jacobian matrix of system (1) at the origin is

$$J = \begin{pmatrix} -\alpha(1 + m_0) & \alpha & 0 \\ 1 & -1 & 1 \\ 0 & -\beta & -\gamma \end{pmatrix}$$

The characteristic equation corresponding to this matrix is

$$\lambda^3 + (\alpha + \gamma + \alpha m_0 + 1)\lambda^2 + (\beta + \gamma + \alpha \gamma + \alpha m_0 + \alpha \gamma m_0)\lambda + \alpha(\beta + \beta m_0 + \gamma m_0) = 0$$

The Routh-Hurwitz conditions for cubic polynomial in the form

$$\lambda^3 + a_1\lambda^2 + a_2\lambda + a_3 = 0$$

are given by

$$a_1 > 0, \quad a_3 > 0 \quad \text{and} \quad a_1 a_2 > a_3.$$

However, the coefficients here are

$$a_1 = \alpha + \gamma + \alpha m_0 + 1, \quad a_2 = \beta + \gamma + \alpha \gamma + \alpha m_0 + \alpha \gamma m_0 \quad \text{and} \quad a_3 = \alpha(\beta + \beta m_0 + \gamma m_0),$$

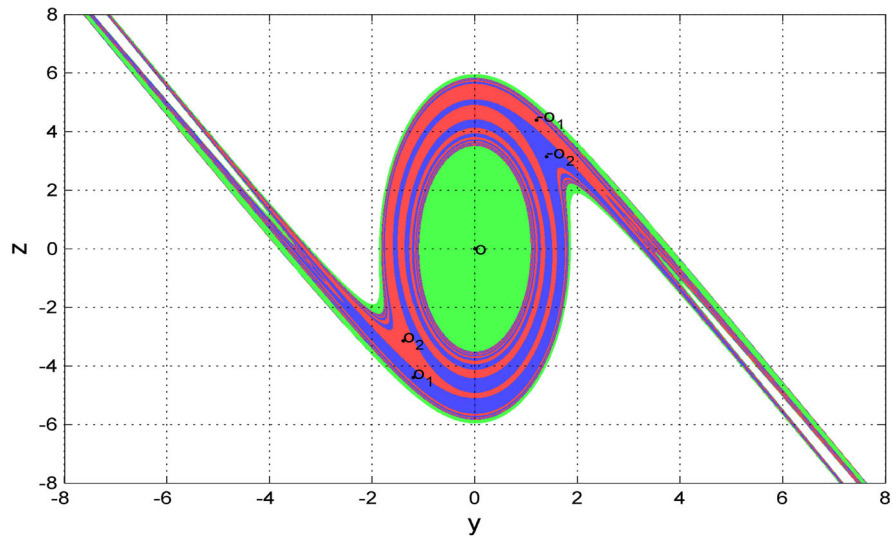
For  $\alpha \in [7.0, 9.0]$ , the first two conditions, i.e.,  $a_1 > 0$  and  $a_3 > 0$ , are satisfied. With the equation, it is not hard to find A critical value  $\alpha_c \approx 8.673$  by numerically solving equation  $a_1 a_2 = a_3$ .

Obviously, when  $\alpha$  is less than  $\alpha_c$ , the origin is stable, so the attractors shown in the bifurcation diagram (Fig. 3) are all hidden; otherwise the attractors in the diagram are not hidden, which can be easily verified by standard simulation procedures mentioned previously.

Now we study the basin of attraction of the Poincaré map to show the relationship of the hidden twin attractors. For clarity, we first investigate the basin of the two periodic limit cycles at  $\alpha = 8.2$ , and then study the basins of other attractors.

Figure 7 shows the basin on the negative half  $yoZ$  plane. In this figure,  $o$ ,  $o_1$  and  $o_2$  indicate the origin and the two period-1 orbits, respectively, and their basins of attraction are illustrated in green, blue, and red color, respectively. Clearly, the basins of  $o_1$  and

**Fig. 8** The whole basin on  $x = 0$  at  $\alpha = 8.2$



$o_2$  is spiraled together, and their boundaries have self-similar patterns, i.e., fractal structures. The basins on the full  $yo_z$  plane is shown in Fig. 8, which suggests that their combination is a multiply connected region, whose inner side is filled by the basin of  $o$ , and whose outer side is surrounded by the basin of  $o$ .

To visualize the basins of attraction and study how they changes, we compute them as we vary  $\alpha$  by the heterogeneous algorithm proposed in [12, 13]. The basic concept is similar to the trapping method used in [23]. For each attractor, we first define a small trapping disk, and discretize a rectangle domain of  $H$  with  $1024 \times 1024$  grid points. Then, we compute the basin of the attractor by checking whether the grid points after a certain times of iteration are inside the disk.

The results are shown in Fig. 9. When  $\alpha = 7.8$ , there is only one period-1 limit cycle, i.e.,  $o_1 = o_2$ , which has a large basin surrounded by the basin of  $o$ . According to Figs. 7 and 8, this basin splits into two basins since the period-1 orbit bifurcates into two different period-1 orbits. And then, the two basins continuously exist during the period-doubling route to chaos. The basins of the two hidden attractor at  $\alpha = 8.4562$  are shown in right-top subfigure in Fig. 9, which looks similar to Fig. 7. When the two hidden attractors become single hidden attractor for some  $\alpha > 8.486$ , their basins merge back together as shown in the bottom-left subfigure in Fig. 9. Since the basin of  $o$  become smaller and smaller as  $\alpha$  increases, it finally disappear at  $\alpha = \alpha_c$ . Then, the system has only a normal chaotic attractor, a typical basin at  $\alpha = 8.8$  is illustrated in the bottom-right sub-

figure in Fig. 9. Numerical study also shows when  $\alpha$  continuously increases, the normal attractor becomes closer and closer to the boundary of its basin, and then disappears when they meet each other at  $\alpha \approx 8.87$ .

### 3 Computer-assisted proof of chaoticity of the hidden attractors

To show that the twin attractors at the parameter  $\alpha = 8.4562$  are not higher periodic orbits as exhibited in the bifurcation process of the usual period doubling bifurcation, we will prove in this section that they are indeed chaotic attractors by means of the topological horseshoe theory.

The topological horseshoe theory, based on the geometric relationship of maps on some subsets of interest in state space, provides a powerful tool in many rigorous studies of chaos, such as estimating topological entropy, proving existence of chaos, showing fractional structure of chaotic invariant sets, revealing mechanism of chaotic attractors and so on. In this section, we first recall a theorem on topological horseshoes, and then present rigorous verification of chaoticity of the three kind of strange attractors illustrated in Fig. 9.

#### 3.1 A result of topological horseshoe

Let  $D$  be a compact connected region of  $R^n$ , and  $D_i, i = 1, 2, \dots, m$  be disjoint compact connected

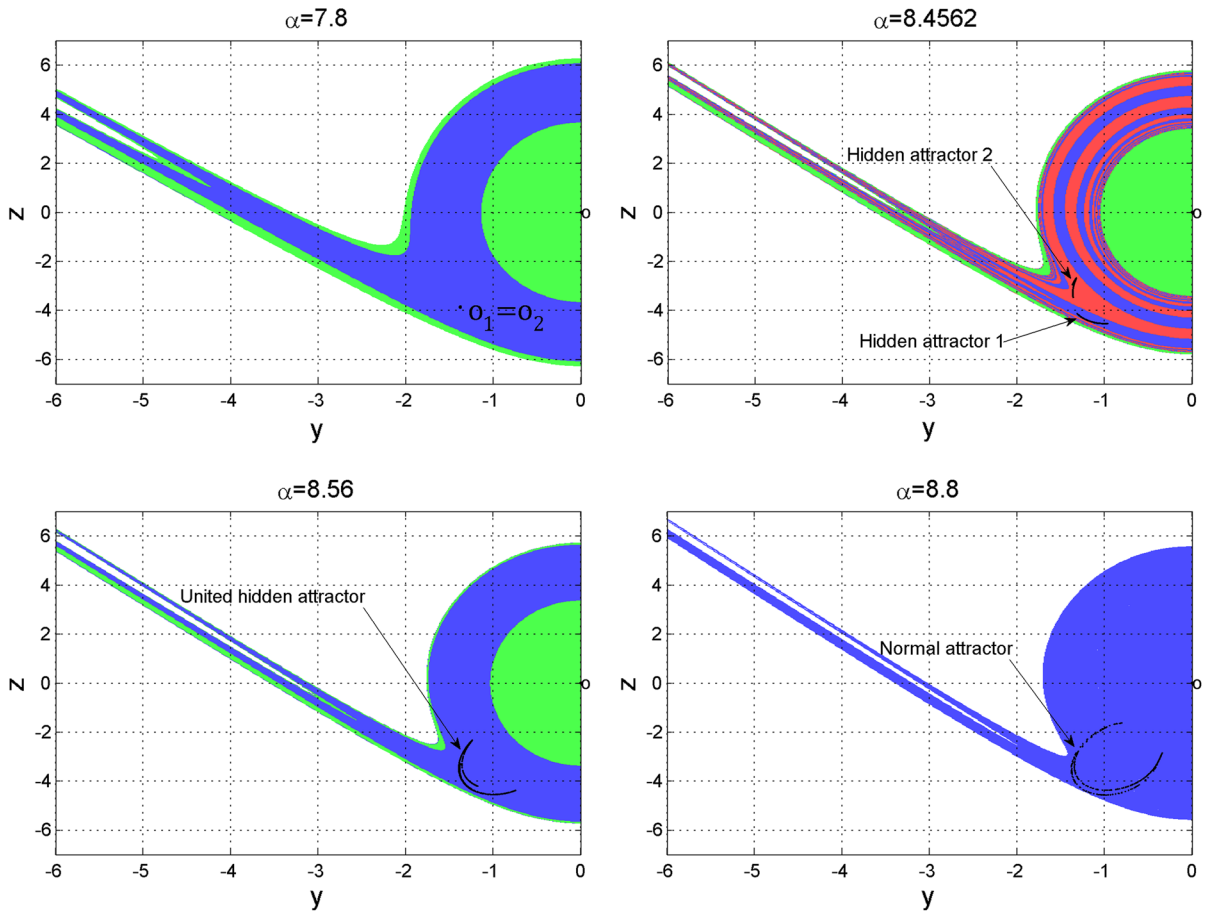


**Fig. 9** The attractors and their basins with adjusting  $\alpha$

subsets (usually quadrangles) of  $D$  homeomorphic to the unit square. Let  $f : D \rightarrow R^n$  be a piecewise continuous map which is continuous on each compact set  $D_i$ , and introduce some concepts and notations as follows.

**Definition 1** [24]. For each  $D_i$ ,  $1 \leq i \leq m$ , let  $D_i^1$  and  $D_i^2$  be two fixed disjoint compact subsets of  $D_i$  contained in the boundary  $\partial D_i$ . A connected subset  $l$  of  $D_i$  is said to connect  $D_i^1$  and  $D_i^2$  if  $l \cap D_i^1 \neq \emptyset$  and  $l \cap D_i^2 \neq \emptyset$ .

**Definition 2** [24]. Let  $l \subset D_i$  be a connection of  $D_i^1$  and  $D_i^2$ . We say that  $f(l)$  is acrossing  $D_j$ , if  $l$  contains a connected subset  $l'$  such that  $f(l') \subset D_j$  is a connection of  $D_j^1$  and  $D_j^2$ . In this case, we denote it by  $f(l) \mapsto D_j$ . Furthermore, if  $f(l) \mapsto D_j$  holds true for every connection  $l$  of  $D_i^1$  and  $D_i^2$  then  $f(D_i)$  is said to be acrossing  $D_j$  and denoted by  $f(D_i) \mapsto D_j$  with respect to two pairs  $(D_i^1, D_i^2)$  and  $(D_j^1, D_j^2)$ .

**Theorem 1** [25]. If the relation  $f(D_i) \mapsto D_j$  holds for every pair with  $i, j$  taken from  $1 \leq i, j \leq m$ , then there exists a compact invariant set  $K \subset D$ , such that  $f|_K$  is semiconjugate to the full  $m$ -shift dynamics  $\sigma|_{\Sigma_m}$ , and  $ent(f) \geq \log m$ .

*Remark* the  $m$ -shift is also called the Bernoulli  $m$ -shift. The symbolic series space  $\Sigma_m$  is the collection of all bi-infinite sequences

$$s = \{\dots, s_{-n}, \dots, s_{-1}; s_0, s_1, \dots, s_n, \dots\},$$

where  $s_i \in \{0, 1, \dots, m-1\}$ . The shift map  $\sigma$  is defined as

$$\sigma(s) = \{\dots, s_{-n+1}, \dots, s_0; s_1, s_2, \dots, s_{n+1}, \dots\}.$$

It is well known that  $\Sigma_m$  is a Cantor set, which is compact, totally disconnected, and perfect. As a dynamical system defined on  $\Sigma_m$ ,  $\sigma$  has: a countable infinity of

periodic orbits consisting of orbits of all periods, an uncountable infinity of aperiodic orbits and a dense orbit. A direct consequence of these three properties is that the dynamics generated by the shift map is sensitive to initial conditions. Mathematically, the topological entropy  $ent(f)$  measures its complexity, which roughly means the exponential growth rate of the number of distinguishable orbits as time advances. When  $m > 1$ ,  $ent(f) > 0$ ; therefore, the system is chaotic. For more details of the above symbolic dynamics and horseshoe theory, we refer the reader to [24–27].

### 3.2 Another Poincaré map

In order to study chaos with the above theorem, we will utilize the technique of cross section and the corresponding Poincaré map. For the convenience of numerical computation, we take the switching manifold

$$\Pi = \{(x, y, z) | x = 1, \dot{x} < 0\}$$

as a new Poincaré section plane. The Poincaré map  $H : \Pi \rightarrow \Pi$  is chosen as follows: For each  $\mathbf{x} = (y, z) \stackrel{\Delta}{=} (1, y, z) \in \Pi$ ,  $H(\mathbf{x})$  is taken to be the first return point in  $\Pi$  under the flow with the initial condition  $\mathbf{x}$ . Since  $f(x)$  is a piecewise linear function, i.e.,

$$f(x) = \begin{cases} m_1x + m_1 - m_0 & 1 < x \\ m_0x & -1 \leq x \leq 1 \\ m_1x - m_1 + m_0 & x < -1 \end{cases},$$

system (1) is a switching system consisted of three linear subsystems:  $S^-$  for  $x < -1$ ,  $S^0$  for  $-1 \leq x \leq 1$ , and  $S^+$  for  $1 < x$ . Clearly, each subsystem has an analytical solution. So it is not hard to compute the image of  $\mathbf{x}$  with reliable bounds of numerical errors by applying interval arithmetic. It is also easy to verify whether  $\Pi$  is continuous on a subset numerically by checking whether the flow of (1) passes through (not tangentially) the switching manifolds  $x = \pm 1$ .

### 3.3 The chaoticity of the twin attractors

To find horseshoes, we need to detect two subsets, e.g.,  $D_1$  and  $D_2$ , such that the relations

$$\begin{aligned} f(D_1) &\mapsto D_1, & f(D_1) &\mapsto D_2, & f(D_2) &\mapsto D_1, \\ f(D_2) &\mapsto D_2 \end{aligned} \tag{5}$$

holds true with respect to two subsets of  $D_1$ , i.e.  $D_1^1$  and  $D_1^2$ , and two subsets of  $D_2$ , i.e.  $D_2^1$  and  $D_2^2$ . Although

this sounds hard, we can use an efficient method proposed in [26], which was realized as a powerful toolbox in MATLAB (available from: <http://www.mathworks.com/matlabcentral/fileexchange/14075>) and has been successfully applied in many planar maps [28, 29] and three-dimensional maps [30, 31].

First, we prove the twin hidden attractors in Fig. 1 is chaotic indeed. Since they are symmetric to each other with respect to the origin, we only prove hidden attractor 1. We numerically find a polygon  $D$  with its ten vertices in term of  $(y, z)$  as follows

$$\begin{aligned} a_1 &= (-0.765271572, -5.526663609), \\ a_2 &= (-0.725104636, -5.527666464), \\ a_3 &= (-0.683240505, -5.523081981), \\ a_4 &= (-0.661176977, -5.518210968), \\ a_5 &= (-0.614221262, -5.504600784), \\ a_6 &= (-0.584803224, -5.490560805), \\ a_7 &= (-0.592723465, -5.489128154), \\ a_8 &= (-0.673057338, -5.511907304), \\ a_9 &= (-0.693989404, -5.514629341), \\ a_{10} &= (-0.782243517, -5.512766895). \end{aligned}$$

The polygon and its image under  $H^2 \stackrel{\Delta}{=} H \circ H$  depict in Fig. 10, where image is so thin that it looks like a line, which passes through the polygon between its top and bottom boundaries, i.e., the piecewise lines  $a_{10}a_9a_8a_7$  and  $a_1a_2a_3a_4a_5a_6$ , and transversely intersects both the left and right boundaries, i.e., the segments  $a_6a_7$  and  $a_1a_{10}$ , twice. The images of  $a_6a_7$  and  $a_1a_{10}$  are both outside of the polygon. This evidence suggests  $H^2|D$  is a Smale horseshoe map. For a detailed study of the horseshoe map with Theorem 1, we can easily take two subsets of  $D$  as shown in Fig. 10, where the first one  $D_1$  is the pentagon  $a_{10}a_1a_2a_3a_9$ , and the two fixed disjoint subsets of  $D_1$  are  $D_1^1$  and  $D_1^2$ , which are the segments  $a_{10}a_1$  and  $a_3a_9$ , respectively; the second one  $D_2$  is the pentagon  $a_8a_4a_5a_6a_7$ , and  $D_2^1$  and  $D_2^2$  are the segments  $a_8a_4$  and  $a_6a_7$ , respectively. The geometrical relationships among  $D_1$ ,  $D_2$  and their images are shown in Fig. 11, from which it is not hard to have the following theorem.

**Theorem 2** *When  $\alpha = 8.4562$ , there exists a compact invariant set  $\Lambda \subset D$ , such that  $H^2|_\Lambda$  is semiconjugate to 2-shift dynamics, and the topological entropy of  $H$  is  $ent(H^2) \geq \log 2$ .*

**Fig. 10** Horseshoe map at  $\alpha = 8.4562$

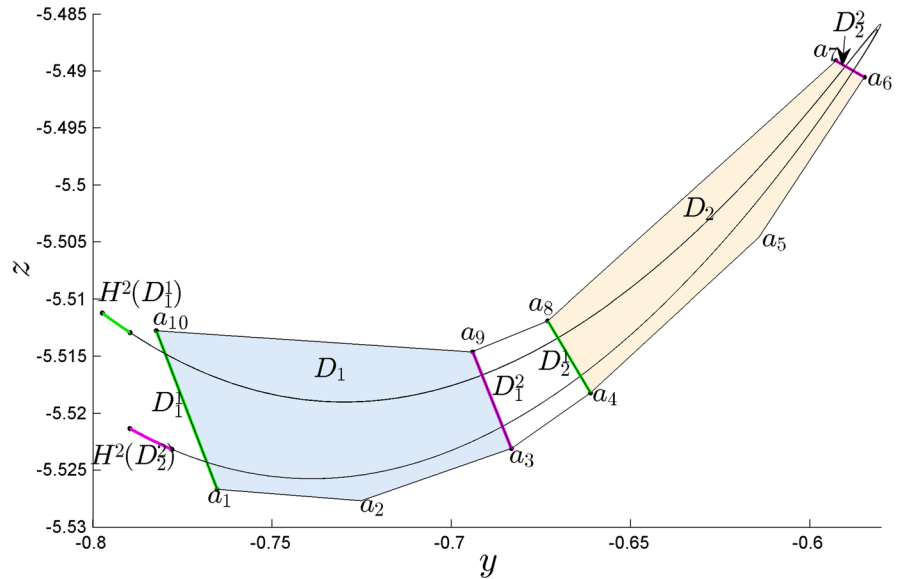
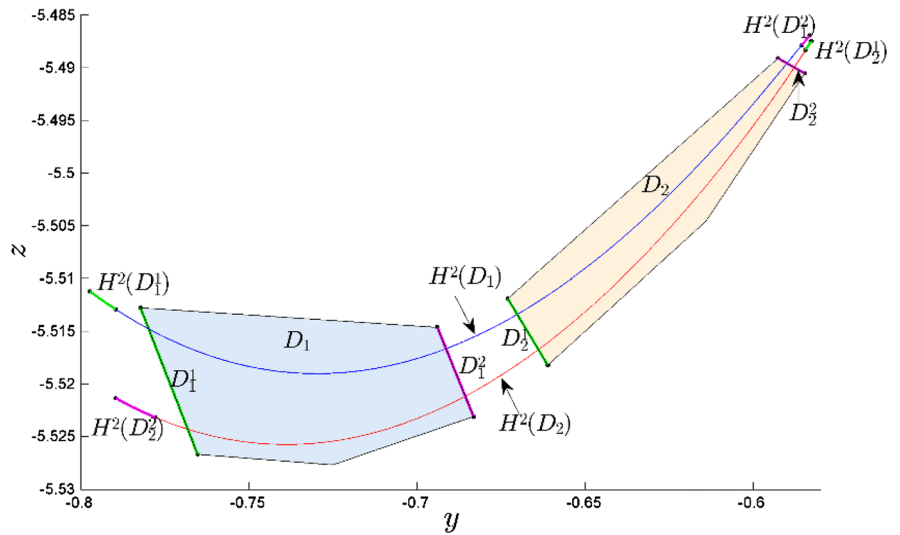


**Fig. 11** Two subset  $D_1$  and  $D_2$  at  $\alpha = 8.4562$



*Proof* According to Theorem 1, we let  $f$  be  $H^2$ , and then we only need to show that the relations (5) hold true.

For the first two relations, it is easy to see from Fig. 11 that  $H^2(D_1)$  passes through  $D_1$  and  $D_2$  between their top and bottom sides, and transversely intersects  $D_1$  with  $D_1^1$  and  $D_1^2$ , intersects  $D_2$  with  $D_2^1$  and  $D_2^2$ . So each connected subset of  $D_1$ , if it is connection of  $D_1^1$  and  $D_1^2$ , then it images under  $H^2$  must be acrossing  $D_1$  with respect to  $D_1^1$  and  $D_1^2$ , and acrossing  $D_2$  with respect to  $D_2^1$  and  $D_2^2$ . Then we have  $H^2(D_1) \mapsto D_1$  and  $H^2(D_1) \mapsto D_2$ .

Similarly, we can prove  $H^2(D_2) \mapsto D_1$  and  $H^2(D_2) \mapsto D_2$  from Fig. 11 too.  $\square$

*Remark* According to the topological horseshoe theory [13], the entropy of the iterated map  $\text{ent}(H^2) = 2 \cdot \text{ent}(H)$ , so the entropy of the original Poincaré map  $H$  is not less than  $\frac{1}{2} \log 2$ .

### 3.4 The chaoticity of the single hidden attractor

Now, we prove that the single hidden attractor in Fig. 9 is chaotic indeed with the same way above. The two

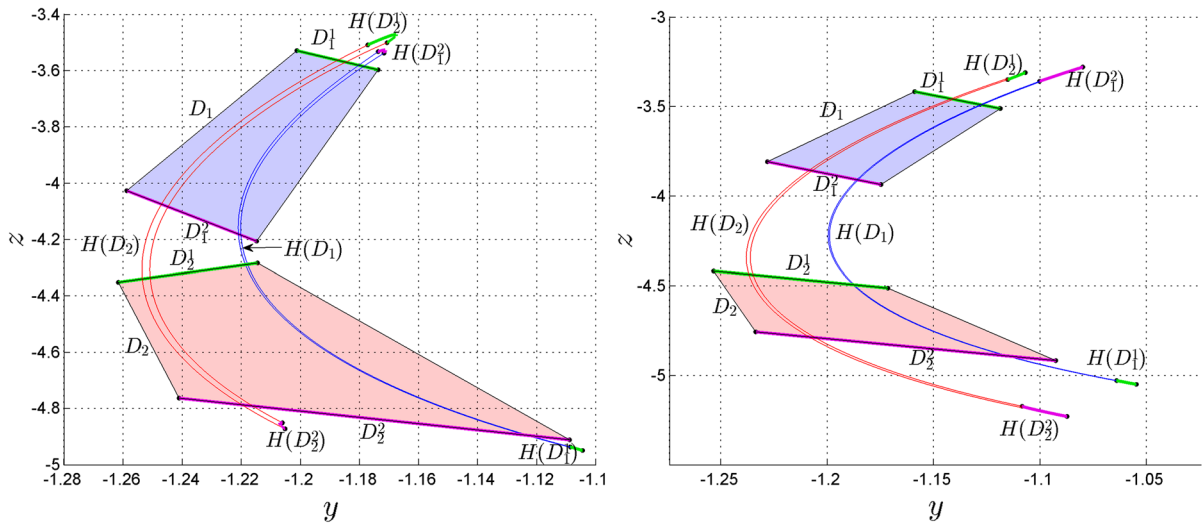


**Fig. 12** Topological horseshoes for the single hidden attractor and the normal attractor

subsets  $D_1$  and  $D_2$  found by us are shown as the left subfigure in Fig. 12, where  $D_1$  is a quadrilateral, whose four vertices in term of  $(y, z)$  are

- $(-1.201194634, -3.531045668),$
- $(-1.173710992, -3.598955096)$
- $(-1.214778503, -4.207053154),$
- $(-1.258689150, -4.028019208)$

And  $D_2$  is also a quadrilateral, whose the four vertices are

- $(-1.261532285, -4.352132387),$
- $(-1.214462599, -4.284222959)$
- $(-1.108950686, -4.910841771),$
- $(-1.240998530, -4.762675746)$

From this figure, we can easily see the following relations

$$\begin{aligned}
 H(D_1) &\mapsto D_1, & H(D_1) &\mapsto D_2, \\
 H(D_2) &\mapsto D_1 & \text{and } H(D_2) &\mapsto D_2.
 \end{aligned}
 \tag{6}$$

which obviously satisfy Theorem 1 if we let  $f$  be  $H$ , so  $ent(H) \geq \log 2$ , which indicates the map is also chaotic indeed when  $\alpha = 8.56$ .

### 3.5 The chaoticity of the normal attractor

At last, we prove that the normal attractor in in Fig. 9 is chaotic too. As shown in the right subfigure in Fig. 12, we find two subsets  $D_1$  and  $D_2$ , which also satisfy the relations (5), where the coordinate of four vertices of  $D_1$  are

- $(-1.159042221, -3.418983312),$
- $(-1.118775145, -3.513511022),$
- $(-1.174873721, -3.937255930),$
- $(-1.228218992, -3.810132458);$

- and the coordinate of four vertices of  $D_2$  are
- $(-1.253496117, -4.419168660),$
  - $(-1.171594743, -4.513765235)$
  - $(-1.092740861, -4.917619842),$
  - $(-1.233687413, -4.757533331).$

According to Theorem 1, the entropy of  $H$  at  $\alpha = 8.8$  is also not less than  $\log 2$ , so the normal attractor is chaotic indeed.

## 4 Conclusions

In this paper we have shown that the so called hidden twin attractors can be observed in the well-known Chua's circuit motivated by the recent remarkable finding of Leonov et al. [6] in the Chua's circuit. To show the chaoticity of the twin attractors we have presented a computer- assisted proof based on the topological horseshoe theory. In addition, we have numerically demonstrated a route from one limit cycle to hidden twin attractors by period-doubling bifurcations. The results of the present paper, together with the previous studies on the Chua's circuit, indicate how rich the dynamics in the Chua's circuit is.

**Acknowledgments** This work is supported in part by National Natural Science Foundation of China (61104150), Science Fund for Distinguished Young Scholars of Chongqing (cstc2013jcyjqq 40001), and the Science and Technology Project of Chongqing Education Commission (No. KJ130517).

## References

- Lorenz, E.N.: Deterministic nonperiodic flow. *J. Atmospheric Sci.* **20**(2), 130–141 (1963)
- Rössler, O.E.: An equation for continuous chaos. *Phys. Lett. A* **57**(5), 397–398 (1976)
- Chua, L.O., Lin, G.-N.: Canonical realization of Chua's circuit family. *IEEE Trans. Circuits Syst.* **37**(7), 885–902 (1990)
- Bilotta, E., Pantan, P.: A gallery of Chua attractors. *Nonlinear Sciences Series A. World Scientific Hackensack, Hackensack* (2008)
- Chen, G., Ueta, T.: Yet another chaotic attractor. *Int. J. Bifurcation Chaos* **9**(07), 1465–1466 (1999)
- Leonov, G.A., Kuznetsov, N.V., Vagitsev, V.I.: Localization of hidden Chua's attractors. *Phys. Lett. A* **375**(23), 2230–2233 (2011)
- Kuznetsov, N., Leonov, G., Vagitsev, V.: Analytical-numerical method for attractor localization of generalized Chua's system. *IFAC Proc. Vol. (IFAC-PapersOnline)* **4**(1), 29–33 (2010)
- Kuznetsov, N., et al.: Analytical-numerical localization of hidden attractor in electrical Chua's circuit. *Informatics in Control, Automation and Robotics*. Springer, Berlin (2013)
- Leonov, G.A., Kuznetsov, N.V., Vagitsev, V.I.: Hidden attractor in smooth Chua systems. *Phys. D* **241**(18), 1482–1486 (2012)
- Bragin, V., et al.: Algorithms for finding hidden oscillations in nonlinear systems. The Aizerman and Kalman conjectures and Chua's circuits. *J. Comput. Syst. Sci. Int.* **50**(4), 511–543 (2011)
- Leonov, G.A., Kuznetsov, N.V.: Hidden attractors in dynamical systems. From hidden oscillations in Hilbert-Kolmogorov, Aizerman, and Kalman problems to hidden chaotic attractor in Chua circuits. *Int. J. Bifurcation Chaos* **23**(01), 1330002 (2013)
- Li, Q., Zhou, H., Yang, X.-S.: A study of basin of attraction of the simplest walking model based on heterogeneous computation. *Acta Phys. Sin* **61**(4), 040503 (2012)
- Li, Q., Yang, X.S.: New walking dynamics in the simplest passive bipedal walking model. *Appl. Math. Model.* **36**(11), 5262–5271 (2012)
- Lozi, R., Ushiki, S.: The theory of confinors in Chua's circuit: accurate analysis of bifurcations and attractors. *Int. J. Bifurcation Chaos* **3**(02), 333–361 (1993)
- Leonov, G.A., Kuznetsov, N.V.: Time-varying linearization and the Perron effects. *Int. J. Bifurcation Chaos* **17**(04), 1079–1107 (2007)
- Kuznetsov, N., Leonov, G.: Stability by the first approximation for discrete systems. *VESTNIK-ST PETERSBURG UNIVERSITY MATHEMATICS C/C OF VESTNIK-SANKT-PETERBURGSKII UNIVERSITET MATEMATIKA.* **36**, 21–27 (2003)
- Chen, T., Choudhury, S.R.: Bifurcations and chaos in a modified driven chen's system. *Far E. J. Dyn. Sys.* **18**(1), 1–81 (2012)
- Gambino, G., Choudhury, S.R., Chen, T.: Modified post-bifurcation dynamics and routes to chaos from double-Hopf bifurcations in a hyperchaotic system. *Nonlinear Dyn.* **69**(3), 1439–1455 (2012)
- Li, Q., Tang, S., Yang, X.-S.: New bifurcations in the simplest passive walking model. *Chaos: an interdisciplinary. J. Nonlinear Sci.* **23**(4), 043110 (2013)
- Gritli, H., Khraief, N., Belghith, S.: Period-three route to chaos induced by a cyclic-fold bifurcation in passive dynamic walking of a compass-gait biped robot. *Commun. Nonlinear Sci. Numer. Simul.* **17**(11), 4356–4372 (2012)
- Chen, Z.-M., Price, W.: Transition to chaos in a fluid motion system. *Chaos, Solitons & Fractals* **26**(4), 1195–1202 (2005)
- Gambino, G., Lombardo, M.C., Sammartino, M.: Adaptive control of a seven mode truncation of the Kolmogorov flow with drag. *Chaos, Solitons & Fractals* **41**(1), 47–59 (2009)
- Boughaba, S., Lozi, R.: Fitting trapping regions for Chua's attractor—a novel method based on isochronic lines. *Int. J. Bifurcation Chaos* **10**(01), 205–225 (2000)
- Yang, X.-S.: Topological horseshoes and computer assisted verification of chaotic dynamics. *Int. J. Bifurcation Chaos* **19**(4), 1127–1145 (2009)
- Yang, X.S., Li, H., Huang, Y.: A planar topological horseshoe theory with applications to computer verifications of chaos. *J. Phys. A* **38**(19), 4175–4185 (2005)
- Li, Q., Yang, X.-S.: A simple method for finding topological horseshoes. *Int. J. Bifurcation Chaos* **20**(2), 467–478 (2010)
- Yang, X.-S., Tang, Y.: Horseshoes in piecewise continuous maps. *Chaos, Solitons & Fractals* **19**(4), 841–845 (2004)
- Fan, Q.J.: Horseshoe chaos in a hybrid planar dynamical system. *Int. J. Bifurcation Chaos* **22**(8), 1250202 (2012)
- Li, Q.D., Yang, X.S., Chen, S.: Hyperchaos in a spacecraft power system. *Int. J. Bifurcation Chaos* **21**(6), 1719–1726 (2011)
- Li, Q., et al.: Hyperchaos and horseshoe in a 4D memristive system with a line of equilibria and its implementation. *Int. J. Circuit Theory Appl.* (2013). doi:[10.1002/cta.1912](https://doi.org/10.1002/cta.1912)
- Li, Q.-D., SongTang, : Algorithm for finding Horseshoes in three-dimensional hyperchaotic maps and its application. *Acta Phys. Sin* **62**(2), 020510 (2013)